WOOD RESEARCH
59 (4): 2014
521-532

EFFECT OF SENSOR NUMBER AND DISTRIBUTION ON ACCURACY RATE OF WOOD DEFECT DETECTION WITH STRESS WAVE TOMOGRAPHY

Shanqing Liang, Feng Fu
Research Institute of Wood Industry Chinese Academy of Forestry
Beijing, China

(Received May 2013)

ABSTRACT

Tomogram accuracy and error rates from different sensor numbers and distributions in defects detection of Euphrates poplar with stress wave tomography were obtained and discussed in this study. Results showed that the accuracy rate would be improved by increasing the number of sensors. For different testing purposes, ten sensors should be used if the investigators hope to obtain a 60 % accuracy rate. However, for obtaining a more accurate defect shape and size, 12 sensors were required, but 22 or more sensors were required to obtain more than a 90 % accuracy rate and an error rate less than 10 %. Tomograms from random, semicircle and an equal sensor distribution with 12 sensors all can detect decayed and hollow areas in tree stems. However, statistical analysis indicated that the accuracy rate does not have a significant difference at the 0.05 confidence level. The results suggest that an equal sensor distribution should be applied if accurately detecting defect shape and size must be obtained in the field.

KEYWORDS: Stress wave tomography, wood, decay, defect detection.

INTRODUCTION

In the past, invasive methods have been applied by investigators to detect the internal defects in wood (Nicolotti et al. 2003, Martinis et al. 2004, Li et al. 2012). However, acoustic tomography is a minimally destructive method for assessing the internal condition of logs and trees (Socco et al. 2004, Lin et al. 2008). Commercial instruments based on stress waves, such as Picus® Sonic Tomography, Arbotom® impulse tomography and Fakopp 2D, have been developed to evaluate internal wood quality (Rabe et al. 2004, Rioux 2004, Wang et al. 2007, Liang et al. 2012a). For stress wave tomography, a set of sensors must be used and connected to the wood by pins to receive stress wave transmissions and calculating time. Using these data, two-dimensional

cross-section tomograms were generated by image reconstruction arithmetic (Gilbert et al. 2004, Schubert et al. 2009). Although the technique can show internal defects, concern about potential disadvantages, which affect the results, need to be overcome for improving assessment accuracy so that stress wave tomography can be widely applied in the field (Zhang et al. 2011). Factors influencing tomograms, including imaging algorithms, tree species, wood structure, sensor number, etc, can all possibly affect the accuracy. For example, the number of test points influenced the minimum detectable defect size. When using four test points the result is 8 %, indicating that a hole occupies 8 % of the cross-sectional area (Divos and Szalai 2002). In fact, there is greater focus on imaging algorithms to increase defect evaluation accuracy, but sensor number and distribution should not be neglected when using multi-channel stress waves to assess tree defects. Although stress wave tomography has the capability to detect severe decay and hollow areas, it cannot reliably detect small sapwood decay, insect holes or crack size (Wang et al. 2009).

The purpose of this study is to provide more fundamental information for stress wave tomography application and use in locating and defining internal defects in wood. Stress wave tomography was applied for evaluating Euphrates poplar defects and discussing sensor number and distribution influence.

MATERIAL AND METHODS

Wood specimens

Eight Euphrates poplar (*Populus euphratica* Oliv.) logs, obtained from Ejna Banner, Inner Mongolia, were used in this study. One disk each, from five of these logs, was cut and air dried to an 8-10 % moisture content to test the effect of sensor quantity in determining defect detection accuracy with stress wave tomography. The disks had either decay or hollow areas in them (Tab. 1).

Tab.1: General character of eight discs.

No.	Testing content		Disc diameter (cm)	Defect type	Defect area (cm^2)
	Sensor number	Sensor distribution			
1	√	√	31.6	Hollow	111.1
2	√	√	30.2	Decay	505.2
3	√		28.7	Hollow	166.6
4	√	√	30.6	Decay	514.3
5	√	√	36.7	Hollow	482.3
6		√	30.1	Hollow	128.4
7		√	28.9	Hollow	132.7
8		√	22.3	Hollow	192.5

** Sign √ means be used to test the influence of sensor

Quantity and distribution of sensors

Stress wave testing was done with an Arbotom® impulse tomography unit, made by Rinntech Inc. Heidelberg, Germany. Initial tests used six sensors to detect defects in the disk specimens. Further tests included 8, 10…., 24 sensors respectively. Pictures were taken of all disks to calculate the defect areas, using Sigma Scan Pro.5 software, following the tomogram readings.

After testing the five discs to determine the number of sensors to be used, four of the five discs were then used to establish sensor spacing distribution. Three more discs were then added in this experiment bringing the total number to seven discs (Tab. 1: disk No. 1, No. 2, No. 4, No. 5, No. 6, No. 7, No. 8, moisture content 8-10 %). The Arbotom® impulse tomography unit, using 12 sensors, was used to test the defects in the wood. Three types of graphs were generated: random (locating the arc length equally between two sensors by sight), semicircle (arc length equally located by calculation for half a cross section, the other half located by sight) and equally distributed (arc length equally located by calculation). The results were analyzed to determine the influence on the tomogram (Tab. 2). The defect areas shown in the tomograms and discs were also calculated by SigmaScan Pro. 5 software, which can accurately calculate the defect area when the dimensions are confirmed by trace code in the software.

Tab. 2: Arc length of two sensors in random, semicircle and equally distributed using 12 testing points.

Disc No.	Distribution type	Arc length of sensor number (cm)											
		1-2	2-3	3-4	4-5	5-6	6-7	7-8	8-9	9-10	10-11	11-12	12-1
	Random	7.7	8.2	8.3	7.9	8.1	7.6	7.7	6.7	7.8	8.5	7.4	8.9
1	Semicircle	7.9	7.9	7.9	7.9	7.9	7.9	5.5	7.5	9.9	7.6	8.6	8.3
	Equal	7.9	7.9	7.9	7.9	7.9	7.9	7.9	7.9	7.9	7.9	7.9	7.9
	Random	8.1	7.5	7.3	11.4	12.6	9.7	8.6	7.1	11.3	10.9	10.4	9.1
2	Semicircle	9.5	9.5	9.5	9.5	9.5	9.5	8.7	9.6	11.6	8.0	10.4	8.7
	Equal	9.5	9.5	9.5	9.5	9.5	9.5	9.5	9.5	9.5	9.5	9.5	9.5
	Random	8.5	8.0	7.8	7.9	8.5	7.3	7.7	8.7	7.6	8.2	8.3	12.3
3	Semicircle	8.4	8.4	8.4	8.4	8.4	8.4	10.3	8.3	7.8	7.4	8.0	8.6
	Equal	8.4	8.4	8.4	8.4	8.4	8.4	8.4	8.4	8.4	8.4	8.4	8.4
	Random	7.0	5.9	7.0	8.7	6.6	7.7	7.0	5.9	7.0	7.2	9.2	10.8
4	Semicircle	7.5	7.5	7.5	7.5	7.5	7.5	9.1	7.1	6.5	9.0	5.5	7.8
	Equal	7.5	7.5	7.5	7.5	7.5	7.5	7.5	7.5	7.5	7.5	7.5	7.5
	Random	6.0	7.9	10.3	9.0	7.5	7.5	7.1	6.9	8.0	11.8	7.8	7.4
5	Semicircle	8.1	8.1	8.1	8.1	8.1	8.1	6.0	7.1	8.0	9.1	9.0	9.4
	Equal	8.1	8.1	8.1	8.1	8.1	8.1	8.1	8.1	8.1	8.1	8.1	8.1
	Random	8.1	7.5	7.3	11.4	12.6	9.7	8.6	7.1	6.9	4.2	5.1	6.3
6	Semicircle	7.9	7.9	7.9	7.9	7.9	7.9	9.1	6.5	7.5	6.2	5.8	12.3
	Equal	7.9	7.9	7.9	7.9	7.9	7.9	7.9	7.9	7.9	7.9	7.9	7.9
	Random	8.5	7.6	4.4	5.6	4.5	4.5	5.4	5.5	6.7	5.2	4.7	7.0
7	Semicircle	5.8	5.8	5.8	5.8	5.8	5.8	4.8	4.2	4.3	7.7	8.3	5.5
	Equal	5.8	5.8	5.8	5.8	5.8	5.8	5.8	5.8	5.8	5.8	5.8	5.8

Data proceeding

The accuracy rate and error rate indices were analyzed to discuss the tomogram accuracy by comparing the discs. Accuracy rate means the defect area percentage between a tomogram and disc:

$$T = \frac{S_t}{S_d} \times 100 \quad (\%) \tag{1}$$

where: S_t - the tomogram defect area,
S_d - the disc defect area.

Error rate means the defect area departure degree between a tomogram and disc. The equation is as follows:

$$V = \frac{S_t - S_d}{S_d} \times 100 \quad (\%) \tag{2}$$

where: S_t - tomogram defect area,
S_d - the disc defect area.

RESULTS

Influence of sensor quantity on tomograms

Fig. 1 shows ten tomograms from disc No. 5 which were generated by stress wave tomography with 6, 8, 10, …, 24 sensors (Total of 50 tomograms in this study. Tomograms from disks No. 1, No. 2, No. 3 and No. 4 will not be shown in this article). In the tomogram, red means decay or hollow area, yellow means light decay and blue is sound wood. The tomogram with 6 sensors shows a large red zone area. However, the tomogram cannot identify the decay shape and size as it provides only minimal information that decay possibly exists in this cross section. Defect shadow and size can be expressed clearly when sensor numbers are increased to 12. The tomograms show that increasing sensor numbers will improve defect detection accuracy.

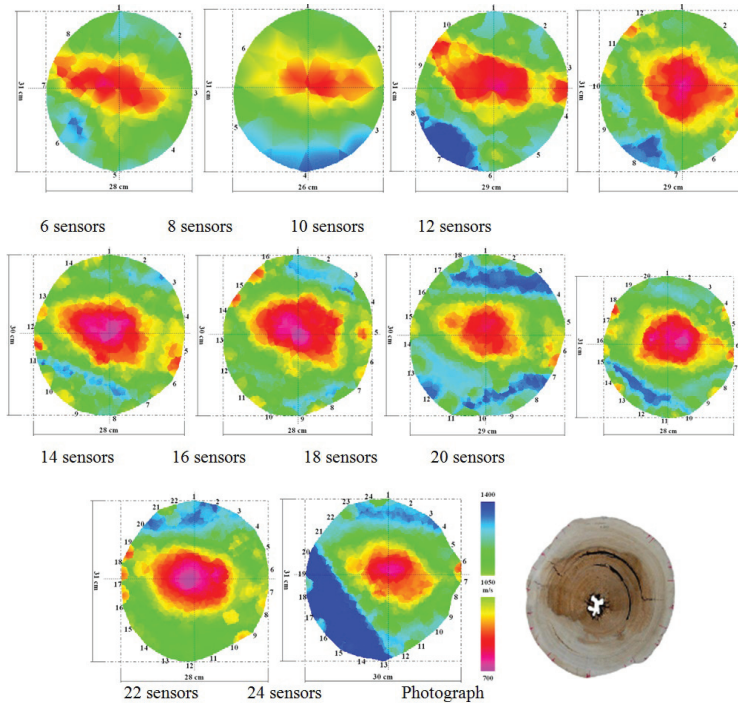

Fig. 1: Tomograms from stress wave tomography with 6, 8, 10, 12, 14, 16, 18, 20, 22, 24 sensors in disc No. 2.

Tomogram defect areas and discs were calculated using SigmaScan Pro.5 software based on the various numbers of sensors that were used for data collection. The accuracy and error rates for the tomograms were also calculated using the same software. Tab. 3 shows accuracy and error rates using different numbers of sensors. Using six sensors, the average accuracy rate was 44 % and average error rate 59 %. In this case, defect location shows low accuracy and an underestimated assessment, but 75.1 % accuracy was found with 12 sensors and a 25 % error rate for all five discs. When sensors increased to 24, the accuracy rate for discs No. 1 and No. 2 was 98.7 and 97.1 %, respectively, but Nos. 3, 4 and 5 were a little higher than 100 % (109.5, 101.3, 109.8 %, respectively). The results confirmed sensor quantity can improve tomogram detection accuracy. However, the defect area shown on the tomogram was different when compared with the disc because determining a defect with color or by sight can lead to a false boundary between decayed and sound wood, thus providing inaccurate values for observers. In the study, for a 22.3-36.7 cm cross sectional diameter range, ten sensors gave investigators a 60 % accurate rate, but 22 or more sensors were necessary if test results required more than 90 % accuracy with less than 10 % error. For different purposes and requirements, testing should be used to select a reasonable sensor quantity to achieve defect assessment, such as to determine if defect location using 10 sensors can meet the requirements. However, to obtain a more accurate defect shape and size, 12 to 22 sensors may be required for higher precision.

Tab. 3: Results of defect area by different sensors.

Disc No.		Sensor number									
		6	**8**	**10**	**12**	**14**	**16**	**18**	**20**	**22**	**24**
1	S_t (cm^2)	53.1	70.2	73.1	86.0	90.3	98.6	104.2	104.7	107.2	109.7
	T (%)	47.8	63.2	65.8	77.4	81.3	88.7	93.8	94.2	96.5	98.7
	V (%)	52.2	36.8	34.2	22.6	18.7	11.3	6.2	5.8	3.5	1.3
2	S_t (cm^2)	161.5	270.9	276.4	448.1	247.9	380.3	289.2	328.6	386.0	490.6
	T (%)	32.0	53.6	54.7	88.7	49.1	75.3	57.2	65.0	76.4	97.1
	V (%)	68.0	46.4	45.3	11.3	50.9	24.7	42.8	35.0	23.6	2.9
3	S_t (cm^2)	114.1	107.9	126.9	143.7	138.5	150.8	148.6	162.6	156.7	182.5
	T (%)	68.5	64.8	76.2	86.2	83.1	90.5	89.2	97.6	94	109.5
	V (%)	31.5	35.2	23.8	13.8	16.9	9.5	10.8	2.4	6.0	9.5
4	S_t (cm^2)	188.3	232.8	376.7	316.0	381.3	401.5	435.3	403.1	479.5	520.9
	T (%)	25.3	45.3	73.2	61.4	74.1	78.1	84.6	78.4	93.2	101.3
	V (%)	90.8	54.7	26.8	38.6	25.9	21.9	15.4	21.6	6.8	1.3
5	S_t (cm^2)	232.3	238.6	260.1	297.9	327.0	338.3	347.1	339.2	464.5	529.5
	T (%)	48.2	49.5	53.9	61.8	67.8	70.1	72	70.3	96.3	109.8
	V (%)	51.8	50.5	46.1	38.2	32.2	29.9	28.0	29.7	3.7	9.8
Total	Average T (%)	44.4	55.3	64.8	75.1	71.1	80.5	79.4	81.1	91.3	103.3
	Average V (%)	59.0	44.8	35.2	25.0	29.0	19.4	20.6	19.0	8.8	5.0

Fig. 2 shows the trend, an accuracy polynomial and the error rate for a different number of sensors. This shows a positive accuracy correlation as the sensor number increases.

Polynomial: $y=0.224x^3-3.8353x^2+23.949x+22.791$, where ($x$=6, 8, 10…, 24), R^2=0.979, y: accuracy rate, x: sensor number.

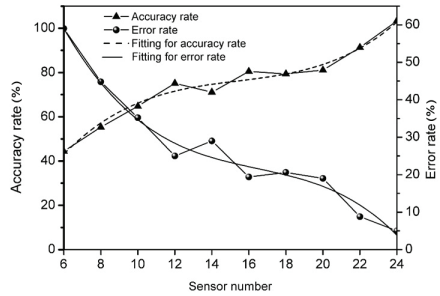

Fig. 2: Correlation between sensor number and accuracy rate or error rate.

In contrast, a negative correlation found error rate as the sensor number increases is: Polynomial: y=-0.207x^3+3.667x^2-23.56x+78.61, where (x=6, 8, 10…, 24), R^2= 0.967, y: error rate, x: sensor number.

Influence of sensor distribution on tomograms

Fig. 3 shows the tomograms from random, semicircle and equally distributed sensors for disc No. 1 to No. 7. Although decay and hollow areas were shown in the tomogram, the defect shadows and sizes showed obvious differences among the three sensor distributions. S_t of No. 1, No. 2, No. 3, No. 4, No. 5 and No. 6 in the random distribution set were higher than the S_t in the semicircle and equally distributed sets, and S_t for disks No. 1 (137.6 cm^2), No. 2 (156.3 cm^2) and No. 5 (203.0 cm^2) were higher than the S_d (111.1 cm^2, 128.4 cm^2, 192.8 cm^2, respectively) for the randomly distributed sensors (Tab. 4). Defect location of equally distributed sensors was more closely predicted to the actual disc when compared with semicircle distributed sensors, but the accuracy rate of equally distributed sensors was not as high as the semicircle and randomly distributed sensors. There are two potential reasons for interpreting these results: First, defect detection with stress wave tomography often underestimated decay or hollow areas in the disc (testing crack overestimates the shadow). Secondly, most of St from random distribution overestimated the defect area which partly compensated the underestimated area so that the accuracy rate increased in certain content. Although the random and semicircle distributed sensors obtained a better accuracy rate than equally distributed sensors, the shape and size of the decay and hollow areas were less accurate than the tomogram made by the equally distributed sensors. These results indicate that the equally distributed sensors should be arranged as described in this study, especially when testing circular and oval shaped tree stems in the field.

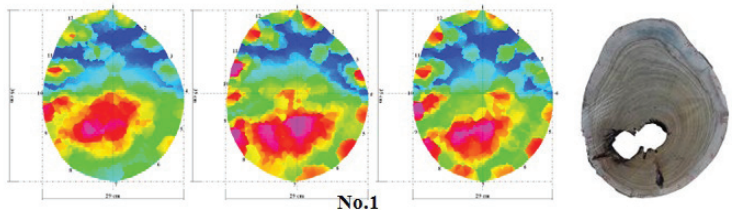

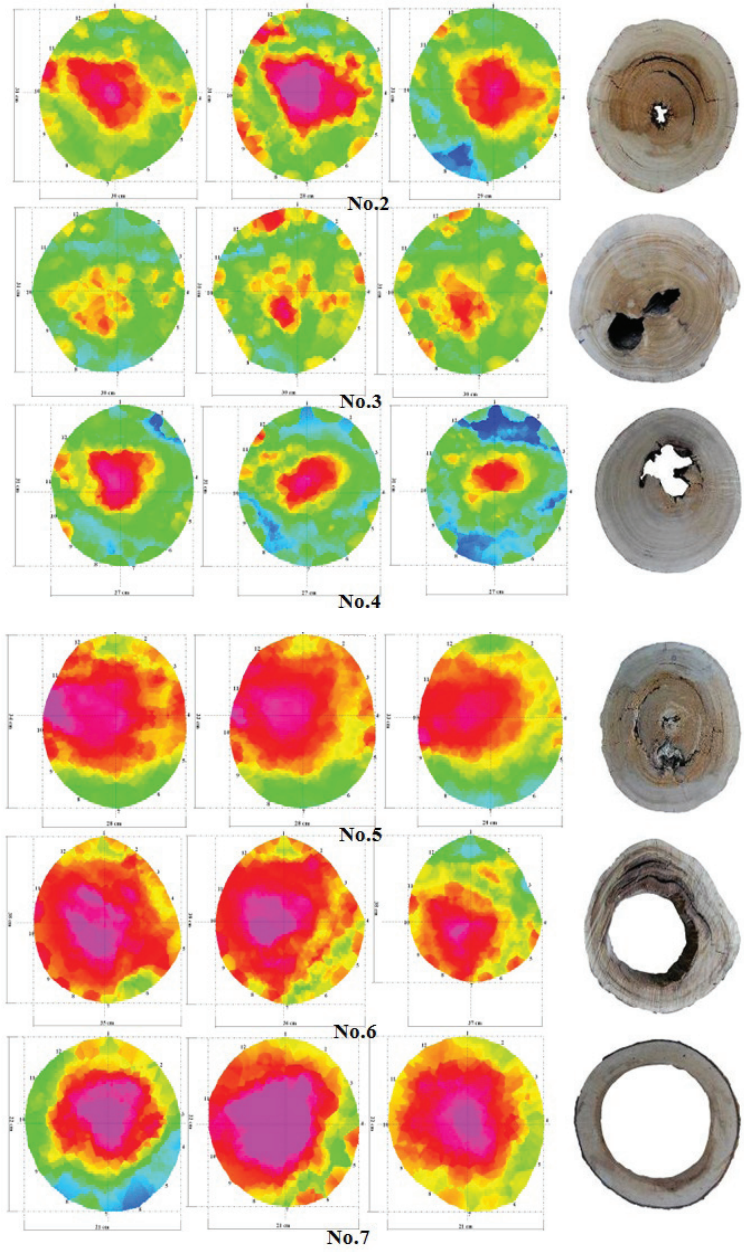

Fig. 3: Tomograms from random, semicircle and equality distributed sensors on disk No. 1 to No. 7 a): Random distribution; b) Semicircle distribution; c) Equality distribution; d) Photograph).

Tab. 4: Defect area of three distribution types and real disc.

NNo.	Random distribution			Semicircle distribution			Equal distribution			S_d (cm^2)
	S_t (cm^2)	T (%)	V (%)	S_t (cm^2)	T (%)	V (%)	S_t (cm^2)	T (%)	V (%)	
1	137.6	123.9	23.9	86.7	78.0	22.0	95.5	86.0	14.0	111.1
2	156.3	121.7	21.7	140.9	109.7	9.7	148.1	115.3	15.3	128.4
3	130.3	98.2	1.8	96.0	72.3	27.7	113.1	85.2	14.8	132.7
4	442.0	93.4	6.6	434.5	91.8	8.2	460.3	97.3	2.7	473.2
5	203.0	105.5	5.5	156.7	81.4	18.6	156.2	81.1	18.9	192.5
6	223.8	83.9	16.1	205.6	77.1	22.9	143.8	53.9	46.1	266.6
7	332.7	58.7	41.3	351.9	62.1	37.9	342.3	60.4	39.6	567.0

Statistical analysis proved that a tomogram defect area using three sensor distributions was not significantly different at the 0.05 confidence level when compared with the disc defect area (F value: 0.2744, Significance: 0.8432). There are also no significant differences among the three distributions based on the multiple comparison results. It was potential suggestion that all three distributions can be used to locate defects if the investigator just wants to get preliminary information. However, equal sensor distribution should be applied if an accurate defect shape and size need to be obtained.

DISCUSSION

Tomography techniques that were developed for engineering or medical applications have been evaluated for their applicability in logs and standing trees. The resolution of images obtained by stress wave based acoustic tomography depends on the acoustic wave frequency, number of sensors used and the applied evaluation algorithm, also affected by pronounced anisotropy of tree species in the terms of microstructures and wood properties. Gilbert and others (2004) applied picus sonic tomography to evaluate the quantification of decay in white oak and hickory, when decay was present, differences between data obtained by the tomogram and actual values were on average 5 %, correlation coefficient between decay area from tomograms and photographs was 0.94, error rate was 2 %, it also reported a high correlation between the amount of decay detected by the stress wave tomography with 12 sensors. The average percentage accuracy for samples where decay was present was 89 %. No cracks were present in the trees they tested. Eight sensors also were used to test the incipient decay, 62 % decay in all disks was successful located, but 8.5% healthy wood be false diagnosed decay wood (Wang et al. 2005). For the number of sensors, our results suggest that the average accuracy rate is obviously improved with increase of sensor numbers (Tab. 3). The accuracy rate was from 44.4 % with 6 sensors increase to 75.1 % with 12 sensors for all discs. According to previous studies, using difference sensor numbers to resolute the hollow tomogram of spruce wood, a relatively quick improvement is observed in the resolution to up to 12 sensors. Above 12, the improvement slows down (Divos and Divos 2005). However, it is not improve the accuracy rate when the decay or hollow area approximately 1cm diameter, even the hollow was not revealed in the tomogram using 12 sensors (Gilbert et al. 2004). It would be beneficial to strategically place more sensors on the critical area of a trunk to improve the local resolution, but increasing the sensor number must be increased the testing time and the cost of detection, it is an important consideration for inspector. The present application of stress wave tomography is most of using 12 sensors to investigate the decay of logs and trees (Deflorio et al.

2008, Wang et al. 2009, Liang and Fu 2012b). It is clear that how many sensors are used to detect the internal defects have to take into account base on the requirement of investigator or the diameter of decay.

The geometries of disks constructed using tomography software generally conformed to the shapes of tree trunks. In other words, sensor distribution is directly related to the geometries of disk. The decay location will be differential shown in tomogram if the geometry of disk is mistake reconstructed so that accuracy rate of defect location will be decreased (Fig. 3). The circular and oval shaped tree stems are easier to construct than the irregular shape using equal distribution methods, that is why equal distribution of sensors usual be applied by investigators. Arbotom® impulse tomography unit can change the sensor distribution to better constructed the shape of trunks, and Picus Sonic Tomograph tool (Argus Electronic Gmbh, Rostock, Germany) offers ellipse and free shapes to measure the geometry of the tree stems (Wang et al. 2008). Considering the complexity of the trunk shape for trees tested, we suggest that selected random distribution method base on irregular shape of tree trunks to construct the geometrical boundary for the tomograms.

CONCLUSIONS

Defect detection results were affected by sensor quantity in stress wave tomography. Tomograms will produce better accuracy results with increased sensor quantity. For different test purposes, ten sensors should be used if investigators hope to obtain a 60 % accuracy rate, 12 sensors to obtain a more accurate defect shape and size, and 22 or more sensors for more than a 90 % an accuracy rate and less than a 10 % error rate. We suggest that sensor numbers should be rationally selected to achieve an accurate assessment of a tree stem.

The tomograms from 12 random, semicircle and equally distributed sensors all effectively showed decay and hollow defects in tree stems in this study, but the accuracy rates were different for the three distribution types. However, statistical analysis indicates that the accuracy rate did not have a significant difference at 0.05 confidence level. The results suggest equally distributed sensors should be applied if accuracy for defect shape and size needs to be obtained in the field. Stress wave tomography can locate internal decay and hollow defects in tree stems, but the defect area displayed by the tomogram was obviously different when compared with the disc. Therefore, it will take more studies to improve tomogram accuracy rate and its testing reliability.

ACKNOWLEDGMENT

The authors are grateful acknowledge financial support from the National Science & Technology Support Program during the Twelfth Five-year Plan Period: Processing Technology Integration and Demonstration of Seldom-used and Low-grade Wood (No.2012BAD24B01).

REFERENCES

1. Deflorio, G., Fink, S., Schwarze, F.W.M.R., 2008: Detection of incipient decay in tree stems with sonic tomography after wounding and fungal inoculation. Wood Science and Technology 42(2): 117-132.

2. Divos, F., Divos, P., 2005: Resolution of stress wave based acoustic tomography. 14th International Symposium on Nondestructive Testing of Wood May 2005, University of Applied Sciences, Germany, Eberswalde. Pp 309-314.
3. Divos, F., Szalai L., 2002: Tree evaluation by acoustic tomography. In: Proceedings of the 13th International Symposium on Nondestructive Testing of Wood. August 19-21, 2002. Berkeley, CA. Pp 251-256.
4. Gilbert, E.A., Smiley, E.T., 2004: Picus sonic tomography for the quantification of decay in white oak (*Quercus alba*) and hickory (*Carya* spp.). Journal of Arboriculture 30(5): 277-280.
5. Liang, S.Q., Fu, F., 2012a: Relationship analysis between tomograms and hardness maps in determining internal defects in Euphrates poplar. Wood Research 57(2):221-230.
6. Liang, S.Q., Fu, F., 2012b: Strength loss and hazard assessment of Euphrates poplar using stress wave tomography. Wood and Fiber Science 44(1): 54-62.
7. Li, L., Wang, X.P., Wang, L.H., Allison, R.B., 2012: Acoustic tomography in relation to 2D ultrasonic velocity and hardness mappings. Wood Science and Technology 46(1): 551-561.
8. Lin, C.J., Kao, Y.C., Lin, T.T., Tsai, M.J., Wang, S.Y., Lin, L.D., Wang, Y.N., Chan, M.H., 2008: Application of an ultrasonic tomographic technique for detecting defects in standing trees. International Biodeterioration & Biodegradation 62(4): 434-441.
9. Martinis, R., Socco, L.V., Sambuelli, L., Nicolotti, G., Schmitt, O., Bucur, V., 2004: Ultrasonic tomography on standing trees. Annual Forest Science 61(2): 157-162
10. Nicolotti, G., Socco, L.V., Martinis, R., Godio, A., Sambuelli, L., 2003: Application and comparison of three tomographic techniques for detection of decay in trees. Journal of Arboriculture 29(2): 66-78.
11. Rabe, C., Ferner, D., Fink, S., Schwarze, F.W.M.R., 2004: Detection of decay in trees with stress waves and interpretation of acoustic tomograms. Arborcultural Journal 28(1-2): 3-19.
12. Rioux, D. A., 2004: A non-invasive acoustic tool revealing decay in trees. Phytoprotection 85(2): 68.
13. Schubert, S., Gsell, D., Dual, J., Motavalli, M., Niemz, P., 2009: Acoustic wood tomography on trees and the challenge of wood heterogeneity. Holzforschung 63(1): 107-112.
14. Socco, L.V., Sambuelli, L., Martinis, R., Cominoa, E., Nicolottib, G., 2004: Feasibility of ultrasonic tomography for nondestructive testing of decay on living trees. Research in Nondestructive Evaluation 15(1): 31-54.
15. Wang, X.P., Allison, R.B., 2008: Decay detection in red oak trees using a combination of visual inspection, acoustic testing, and resistance microdrilling. Arboriculture & Urban Forestry 34(1): 1-4.
16. Wang, X.P, Allison, R.B., Wang, L.H, Ross, R.J., 2007: Acoustic tomography for decay detection in red oak trees. Gen. Tech. Rep. FPL-GTR-642. Madison, WI: U.S. Department of Agriculture, Forest Service, Forest Products Laboratory, 7 pp.
17. Wang, X.P., Wiedenbeck, J., Liang, S.Q., 2009: Acoustic tomography for decay detection in Black Cherry trees. Wood and Fiber Science 41(2): 1-11.
18. Wang, X.P., Wiedenbeck, J., Ross, R. J., Forsman, J.W., Erickson, J.R., Pilon, C., Brashaw, B.K., 2005: Nondestructive evaluation of incipient decay in hardwood logs. Gen. Tech. Rep. FPL-GTR-162. Madison, WI: U.S. Department of Agriculture, Forest Service, Forest Products Laboratory, 11 pp.
19. Zhang, H.J., Wang, X.P., Su, J., 2011: Experimental investigation of stress wave propagation in standing trees. Holzforschung 65(5): 743-748.

Liang, Fu
Research Institute of Wood Industry, Chinese Academy of Forestry
Xiangshan Road
Haidian District
Beijing 100091
Phone: +86 10-62889241
China
Corresponding auhor: liangsq@caf.ac.cn